

## Small-Angle Scattering Study of Short Pendant Chain Perfluorosulfonated Ionomer Membranes

Gérard Gebel\*

CEA/Grenoble, Département de Recherche Fondamentale sur la Matière Condensée, SI3M-Groupe Polymères Conducteurs Ioniques, 17, rue des Martyrs 38054 Grenoble, Cedex 9, France

Robert B. Moore

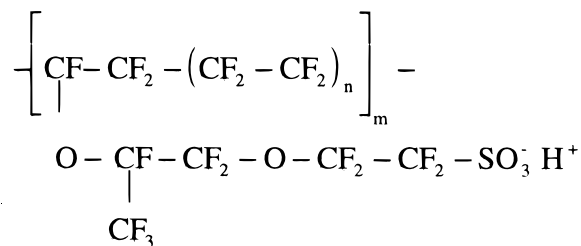
Department of Polymer Science, University of Southern Mississippi, P.O. Box 10076, Hattiesburg, Mississippi 39406-0076

Received July 30, 1999

**ABSTRACT:** A structural study using both small-angle X-ray and neutron scattering (SAXS and SANS) of dry and water-swollen short pendant side chain perfluorosulfonated ionomer (SPC PFSI) membranes is presented. The SAXS and SANS profiles are shown to be equivalent, confirming the phase separation between the water and the perfluorinated matrix. The study of the asymptotic behavior at large angles of the scattering curves confirms that the structure is dominated by the polymer–solvent interfacial energy. The local order model is shown to satisfactorily reproduce the scattering profiles obtained for SPC PFSI membranes depending on the equivalent weight (EW) with a low number of free parameters. However, the values of the parameters for large EWs are not in agreement with those determined from the Porod analysis due to the presence of a well-defined maximum at low  $q$  values. This maximum, attributed to a crystalline component, slightly modifies both the position and the intensity of the ionomer peak. For the low EW membrane, which generates a very large water uptake, we propose to describe the swollen membrane as a connected network of rods.

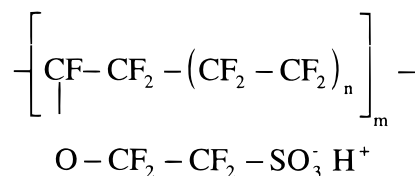
### Introduction

Perfluorosulfonated ionomer (PFSI) membranes were first developed for applications as separators in chlor-alkali electrolyzers.<sup>1–3</sup> The foremost PFSI membrane was commercialized by duPont de Nemours under the trade name Nafion and corresponds to a long pendant chain perfluorosulfonated ionomer (LPC PFSI):



These membranes were shown to be characterized by a microphase separation between the ionic domains and the polymer matrix, which gives rise to a small-angle scattering maximum, called the “ionomer peak”.<sup>4,5</sup> In swollen membranes, the water was shown to be localized in water pools<sup>6</sup> embedded in the polymer matrix with the ionic groups principally located at the polymer–solvent interface.<sup>7</sup> A recent work on water-swollen LPC PFSI membranes using both small-angle X-ray and neutron scattering (respectively SAXS and SANS) techniques revealed that the local order model was the only proposed model able to reproduce satisfactorily the shape of the scattering maximum on the absolute scale of scattered intensities with a very low number of free parameters.<sup>8</sup> This model is based on the hypothesis that each ionic aggregate is spherical and surrounded by four aggregates (tetrahedral coordination) at a well-defined distance while the following ionic domains are considered to be randomly distributed.<sup>9</sup>

To improve the ion conduction properties and the cation versus anion permselectivity, several developments of the membrane structure were then proposed, including the introduction of carboxylated ionic groups<sup>1</sup> or the synthesis of short pendant side chain perfluorosulfonated ionomers (SPC PFSI).<sup>10,11</sup>



While many structural studies have been devoted to LPC PFSIs, only a few studies have appeared that focus on swollen SPC PFSI membranes.<sup>11–13</sup> The SAXS profiles of EW = 800 g/equiv SPC and the EW = 1100 g/equiv LPC water-swollen PFSI membranes, where EW is the equivalent weight, present roughly the same shape and the same peak position. This result was considered as an indication that the same cluster size yet a different cluster density is obtained for these membranes.<sup>13</sup> Over a comparable range of equivalent weights, wide-angle X-ray scattering studies revealed a higher degree of crystallinity for SPC PFSI compared to LPC PFSI.<sup>11,12</sup> Using a modified plot of the SAXS scattered intensity, which effectively restrains the effect of the strong upturn in intensity at low angles, Moore et al. suggested the existence of a crystalline contribution to the scattering profiles for the SPC PFSI systems.<sup>11</sup> Nevertheless, since these previous SAXS studies of SPC PFSI were focused primarily on the ionomer peak, and the scattering from the crystalline domains is expected to be observed only at very low angles superimposed on the intense small-angle upturn, a

**Table 1. Polymer Characteristics and Water Uptakes<sup>a</sup>**

EW	635	803	909	1076	1269
$n$	3.6	5.25	6.3	8.0	9.9
$v_0$ (Å <sup>3</sup> )	502	634	719	851	1003
$f$ (%)	190	37.5	22.7	15.9	12.5
$\phi_w$ (%)	79.2	42.9	31.2	24.1	20.0
$\lambda$ (H <sub>2</sub> O/SO <sub>3</sub> )	63.7	15.9	10.9	9.0	8.3

<sup>a</sup> EW is the equivalent weight (g/equiv),  $n$  is the average number of tetrafluoroethylene repeat units in the polymer backbone,  $v_0$  is the average volume associated with each ionic group,  $f$  is the w/w water uptake,  $\phi_w$  is the water volume fraction in the swollen membranes, and  $\lambda$  is the number of water molecules per SO<sub>3</sub> group.

detailed interpretation of the crystalline contribution was limited.

The present work is devoted to the analysis of the SAXS and SANS data of SPC PFSI membranes over an extended angular range. At low angles, the existence of a scattering maximum related to the crystallinity will be evaluated. The asymptotic behavior at large angles of the scattering curves will be analyzed in order to extract a value of the area per polar headgroup (i.e., the pendent sulfonate ion). In the intermediate range, the ability of the local order model to reproduce the ionomer peak with variable equivalent weights of the membranes will be considered.

## Experimental Section

The SPC PFSI membranes were obtained from Dow Chemical Co. The EW values, the average number of CF<sub>2</sub> units between two pendant side chains ( $n$ ), the average polymer volume per ionic group ( $v_0$ ), the degree of swelling ( $f$ ), the water volume fraction ( $\phi_w$ ), and the number of water molecules per ionic group ( $\lambda$ ) are listed in Table 1.

Prior to analysis, the membranes were cleaned in boiling concentrated nitric acid for 1 h, neutralized using a 1 M NaOH (or LiOH) solution, and rinsed several times with pure water. The membranes were equilibrated in water for at least 5 h, and the water uptake was determined by weighing.

The SANS experiments were performed at the Laboratoire Léon Brillouin (CEA/CNRS, Orphée reactor, Saclay, France) on the PAXE spectrometer. The overall angular range ( $5 \times 10^{-3} < q$  (Å<sup>-1</sup>)  $< 0.3$  with  $q = 4\pi \sin \theta/\lambda$  where  $\theta$  is the scattering angle) was accessed varying the wavelength from  $\lambda = 5$  Å to  $\lambda = 12$  Å and the sample-to-detector distance from 1.2 to 5 m. The samples were placed in quartz cells with a 1 mm path length. Usual corrections for the incoherent background subtraction and absolute scale normalizations were applied to the data.

The SAXS profiles for the SPC PFSI membranes varying the equivalent weight were recorded on the Oak Ridge National Laboratory 10 m SAXS system with a 2-dimensional position-sensitive proportional counter as previously described.<sup>11</sup> Both SANS and SAXS experiments were performed using focused beams that allow the use of a pinhole collimation approximation.

## Small-Angle Scattering Background

The asymptotic behavior at large angles of the scattering curve reflects the nature of the interface. For a sharp polymer-solvent interface, the asymptotic behavior of the scattering curves is related to the quantity of interface through the relation<sup>14</sup>

$$\lim_{q \rightarrow \infty} q^4 I(q) = 2\pi(\Delta\rho)^2 \Sigma = \frac{\Sigma \text{INV}}{\pi\phi(1-\phi)} \quad (1)$$

where  $\Sigma$  is the total surface-to-volume ratio,  $\Delta\rho$  is the scattering length density difference between the perfluorinated matrix and the solvent,  $\phi$  is the water

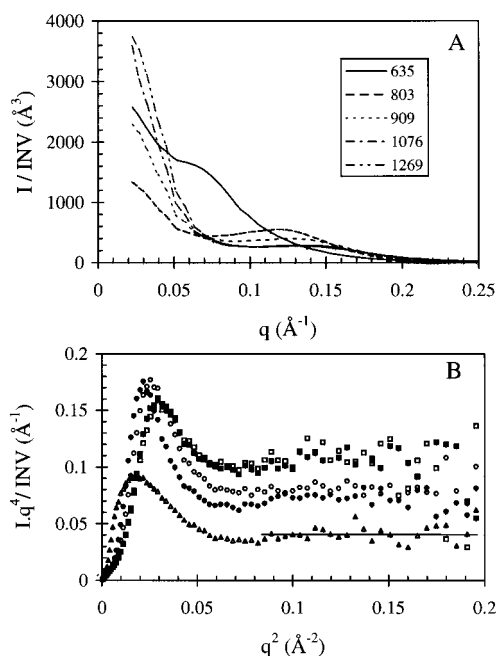


**Figure 1.** (A) SAXS profiles of Na<sup>+</sup> SPC PFSI membranes. (B) Porod plot of the same data EW = 635 (Δ), 803 (●), 909 (○), 1076 (■), and 1269 (□).

volume fraction, and INV is the scattering invariant defined as

$$\text{INV} = \int_0^\infty q^2 I(q) dq = (\Delta\rho)^2 \phi(1-\phi) 2\pi^2 \quad (2)$$

The scattering invariant is useful to normalize the intensities and to avoid any hypothesis on the contrast such as the quantity of ion pairs embedded in the perfluorinated matrix. The area per polar headgroup at the polymer solvent interface,  $\sigma$ , can be deduced from  $\Sigma$  by introducing the average volume per ionic group,  $v_0$ , and the water volume fraction,  $\phi_w$ :

$$\sigma = \frac{v_0 \Sigma}{1 - \phi_w} \quad (3)$$

It should be noted that the calculated neutron and X-ray contrast terms,  $\Delta\rho$ , are very close for water-swollen PFSI membranes ( $\Delta\rho_{\text{neutron}} = 5.3 \times 10^{10} \text{ cm}^{-2}$  and  $\Delta\rho_{\text{X-ray}} = 5.6 \times 10^{10} \text{ cm}^{-2}$ ).

The local order model is based on the following hypotheses: the ionic aggregates are spherical, the first four neighbors of each aggregate are located at a well-defined distance  $D$ , and the ionic domains at a distance larger than  $\alpha D$  are randomly distributed. This hypothesis was depicted in a radial pair distribution function presenting a correlation hole containing four particles in a Dirac peak at the distance  $D$  (Figure 1). The scattered intensity can then be expressed as<sup>8,9</sup>

$$\frac{I(q)}{\text{INV}} = \frac{2R^3}{3(1-\phi_w)\pi} \Phi(qR)^2 \left( 1 + 4 \frac{\sin(qD)}{qD} - z\Phi(\alpha qD) \right) \quad (4)$$

where  $R$  is the cluster radius,  $D$  is the distance between clusters,  $\alpha D$  is the size of the correlation hole defined in the distribution function, and  $z$  is the number of ionic aggregates "missing" in the pair distribution function due to the existence of the correlation hole. The  $\Phi(x)$

function is defined as

$$\Phi(x) = 3 \frac{\sin(x) - x \cos(x)}{x^3} \quad (5)$$

The hypothesis of a tetrahedral coordination combined with space-filling arguments provides a relation between the interaggregate distance and their radius:

$$D = \left( \frac{\sqrt{3}\pi}{2\phi_w} \right)^{1/3} R \quad (6)$$

Since the radius can be deduced from the asymptotic behavior at large angles, the only free parameters of the model are  $\alpha$  and  $z$ .

## Results

The SAXS profiles obtained for various water-swollen membranes with different EW values are presented in Figure 1A. The ionomer peak shifts significantly toward smaller  $q$  values as ionic content increases due to the increase in water uptake. The number of water molecules per ionic group increases with ionic content,<sup>10</sup> which leads to larger ionic domains and interdomain distances. These data were previously presented on a Kratky plot ( $Iq^2$  vs  $q$ ) using relative intensities, which tend to emphasize the ionomer peak with respect to the small-angle upturn in intensity.<sup>11</sup> The same data normalized by the scattering invariant presented on a  $I(q)$  vs  $q$  plot exhibit several different features: (i) the profiles obtained for the EW = 1096 and the EW = 1269 membranes are almost identical for a  $q$  value larger than  $0.08 \text{ \AA}^{-1}$  except that a more intense small-angle upturn is observed for the EW = 1269 sample (due to a larger contribution of the crystalline component); (ii) the Kratky representation reveals a second scattering maximum at low  $q$  values for high equivalent weight membranes which is hardly discernible on a  $I$  vs  $q$  plot; (iii) the intensity of the ionomer peak increases continuously with decreasing equivalent weight, while the previous representation indicated a lower intensity for the EW = 635 membrane attributed to the fact that the volume fraction of the ionic phase exceeds the volume fraction of the polymer phase.

The data presented on a Porod representation ( $Iq^4$  vs  $q^2$ ) exhibit a constant behavior at large  $q$  values, which indicates the existence of a sharp polymer-solvent interface (Figure 1B). Despite the moderate scatter in the data at high  $q$  values, the Porod limit can be easily extracted and provides a value for the quantity of interface for each membrane. The values of the specific areas calculated from the quantity of interface according to eq 3 are reported in Table 2. Regardless of the large water content variation depending on the equivalent weight, the values of the specific surface are relatively constant. This result confirms the fact that the structure is dominated by interfacial phenomena. The value of the area per polar headgroup deduced from the Porod limit is not model dependent except for the reasonable assumption that all the water molecules are predominately located within the ionic domains. The average value,  $\sigma = 61 \text{ \AA}^2$ , is smaller than the value obtained for SPC PFSI solutions ( $70\text{--}74 \text{ \AA}^2$ )<sup>15</sup> and is slightly larger than the value obtained for LPC PFSI swollen membranes ( $\sigma = 55 \text{ \AA}^2$ ).<sup>8,16</sup> Since the relevant parameter is the polymer-solvent interfacial energy, the system will try to minimize its free energy by forming spherical ionic

**Table 2. Results from the Small-Angle Scattering Analysis<sup>a</sup>**

	635	803	909	1076	1269
EW	635	803	909	1076	1269
$\sigma$ ( $\text{\AA}^2$ )	58	60	58	64	63
$R_\Sigma$ ( $\text{\AA}$ )	100	24	17	13	12
$N_\Sigma$	2167	121	63	33	29
$d_{\max}$ ( $\text{\AA}$ )	90	52.4	48.3	44.9	44.9
$R$ ( $\text{\AA}$ )		21.4	19.3	18	17.5
$D$ ( $\text{\AA}$ )		39.0	39.7	40.4	41.8
$\alpha$		1.152	1.163	1.175	1.19
$z$		4.75	4.5	4.1	4.1

<sup>a</sup>  $\sigma$  is the area of interface per polar head group,  $R_\Sigma$  and  $N_\Sigma$  are respectively the radius and the number of ionic groups per aggregates deduced from the Porod analysis,  $d_{\max}$  is the peak position,  $R$  is the radius deduced from the analysis using the local order model,  $\alpha$  and  $z$  are two fit parameters defining the radial distribution function, and  $D$  is the calculated interaggregate distance.

aggregates. It has been shown that the conservation of the area per polar headgroup with swelling combined with the maximum distance between two ionic groups along the polymer chain favors the percolation of the ionic domains at rather low water contents.<sup>17</sup>

A value of the radius,  $R_\Sigma$ , was determined for each membrane from the quantity of interface deduced from the Porod analysis and is reported in Table 2. From the swelling data reported in Table 1, it can be shown that the  $\lambda$  values diverge at low ionic contents, which allows for a prediction of polymer dissolution for an EW lower than ca. 500. For the EW = 635 membrane, the water volume fraction is extremely large ( $\approx 80\%$ ), and it is no longer possible to conform to the packing constraints assuming the existence of spherical ionic domains. In such a case, it was recently shown with LPC PFSI that the structure has to be considered as a connected network of rodlike polymer aggregates.<sup>16</sup> The other interesting result deduced from the swelling data is that a  $\lambda$  value close to 8 can be extrapolated at infinite equivalent weight. Since both  $\sigma$  and  $\lambda$  are constant at large EW, a minimum value of the radius can be determined,  $R = 12 \text{ \AA}$ , dividing the aggregate surface by its volume and assuming that the volume of a water molecule inside the aggregate is  $30 \text{ \AA}^3$ :

$$R_\Sigma = \frac{90\lambda}{\sigma} \quad (7)$$

In addition, it is possible to calculate the number of ionic groups per cluster,  $N_\Sigma$ , combining the value of the radius and the area per polar headgroup:

$$N_\Sigma = \frac{4\pi R_\Sigma^2}{\sigma} \quad (8)$$

The SANS profiles obtained for a room temperature water-swollen ( $\phi_w = 0.43$ ) and a room humidity equilibrated ( $\phi_w = 0.13$ ) membrane are presented in Figure 2 over an extended angular range. The main result from these data is that the SANS curves present two well-defined scattering maxima. The low  $q$  maximum ( $q_{\max} \approx 0.02 \text{ \AA}^{-1}$ ) was not fully explored in previous SAXS studies of SPC PFSI because the limited angular domain was focused on the scattering maximum attributed to the ionic domains, and inadequate data were obtained on the behavior of the scattering curves at low angles. The scattering maximum located at large  $q$  values ( $q_{\max} \approx 0.15 \text{ \AA}^{-1}$ ) corresponds to the well-known "ionomer peak" while the scattering maximum located



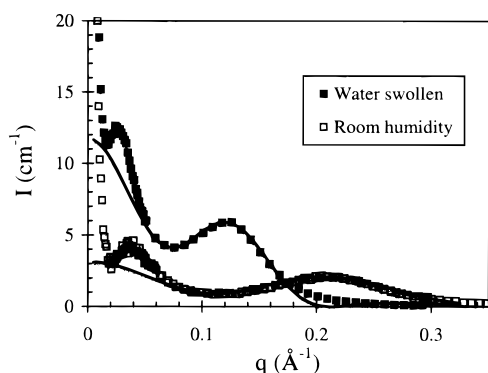


**Figure 2.** SANS profiles of EW = 800 SPC PFSI equilibrated at room humidity  $\phi_w = 0.14$  ( $\square$ ) and with liquid water  $\phi_w = 0.43$  ( $\blacksquare$ ). The solid lines correspond to the best fits using the local order model.

at low  $q$  values can be attributed to a crystalline component related to the long period between the lamellar crystallites.<sup>5,7,18,19</sup> The existence of crystallinity in the EW = 800 SPC polymer was previously evidenced by both wide-angle X-ray scattering and differential scanning calorimetry experiments.<sup>11</sup> The long period deduced from the peak position for EW = 800 SPC PFSI equilibrated with room humidity ( $L \approx 160$  Å) is similar to the one encountered with thermally annealed solution cast EW = 1100 LPC PFSI ( $L \approx 150$  Å).<sup>20</sup> Since LPC PFSI membranes do not exhibit crystallinity for EW values lower than 1000 (as observed by wide-angle X-ray scattering), the existence of a well-defined crystalline component in the small-angle scattering curve for the EW = 800 SPC PFSI confirms the higher level of crystallinity observed by reducing the pendant side chain length. This behavior was attributed to the fact that the shorter pendant side chains disrupt to a lesser extent the crystalline arrangement of the PTFE segments.<sup>11</sup> However, since both the average number of CF<sub>2</sub> units between two lateral chains ( $n = 5.25$ ) and the average volume of polymer associated with an ionic group ( $v_0 = 634$  Å<sup>3</sup>) are smaller for the EW = 800 SPC PFSI compared to the EW = 1100 LPC PFSI ( $n = 6.45$ ,  $v_0 = 870$  Å<sup>3</sup>), it is more reasonable to expect a lower degree of crystallinity for the SPC PFSI. Thus, in agreement with the previous study of these ionomers, it is apparent that the higher crystallinity index observed for SPC PFSI is indication that the copolymerization is not statistical, such that a significant fraction of long run length PTFE segments exists in the polymer microstructure.<sup>11</sup>

One of the most interesting features of the SANS data in Figure 2 is that the low  $q$  maximum is still observable and well-defined in the SANS profile of the water-swollen membrane containing 43 vol % water. This indicates that solvent swelling does not appreciably disrupt the crystalline domains. Moreover, the shift of this scattering maximum from 0.038 to 0.025 Å<sup>-1</sup> is proportional to the water volume fraction increase from  $\phi = 0.13$  to  $\phi = 0.43$ , which follows that expected for the swelling of a lamellar structure. In contrast to this swelling behavior, the shift of the ionomer peak maximum (from 0.212 to 0.123 Å<sup>-1</sup>) is significantly different. Therefore, the dissimilar shifts of the two maxima as water content increases are not in agreement with the model proposed by Litt,<sup>21</sup> which essentially stipulates a parallel shift for the two maxima attributed to a lamellar structure of the ionic domains imposed by the semicrystalline character of the polymer.

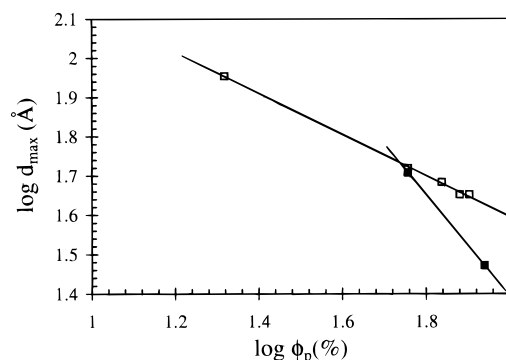


**Figure 3.** Iononmer peak position vs polymer volume fraction: effect of swelling EW = 800 ( $\blacksquare$ ) and effect of variation in EW ( $\square$ ).

The peak position,  $q_{\max}$ , can be related to a Bragg distance,  $d_{\max}$ , through the relation  $d_{\max} = 2\pi/q_{\max}$ . The evolution of the Bragg distance against the polymer volume fraction is presented in a double-logarithmic plot (Figure 3). By varying the ionomer EW, a linear trend with a slope equal to  $-0.5$  is observed for the water-swollen membranes. However, for a single EW (e.g., the EW = 800 membrane), a simple variation in the water content by solvent swelling yields a plot that exhibits a significantly different slope ( $-1.3$ ), which is very close to that determined for LPC PFSI ( $-1.33$ ).<sup>16</sup> The two scaling laws are attributable to polymer reorganization upon swelling. The area of water-polymer interface per polar headgroup is independent of both the water content<sup>16</sup> and the equivalent weight (Table 2). By increasing the water content, the volume of the ionic domains increases, inducing an increase of the number of ionic groups per domain to maintain constant the area per polar headgroup. Therefore, the total number of domains decreases, and the interdomain distance increases significantly more than what would be expected for an affine swelling behavior (slope =  $-0.33$ ). The scaling law obtained for the swelling of EW = 800 SPC PFSI thus reflects the geometrical constraints associated with the swelling (elastic energy of the polymer chains, interfacial energy, osmotic pressure, etc.) and the geometrical arrangement of the domains. The scaling law obtained by varying the EW value also involves a corresponding change in the water content, yet it is significantly lower than that of the simple swelling behavior. This indicates a smaller degree of polymer reorganization (less variation of the interdomain distance) due to the fact that ionic groups are added in addition to water molecules, and the structural modification necessary to maintain a constant area of interface per polar headgroup is thus minimized.

The SAXS and SANS profiles normalized by the scattering invariant obtained for an EW = 800 SPC PFSI are exactly superimposable over the entire angular range, indicating that the system can be analyzed as a true two-phase system despite the presence of crystallites. This result was already observed for LPC PFSI for both membranes<sup>8</sup> and solutions<sup>22</sup> and confirms the phase separation between the solvent and the perfluorinated matrix. The  $q$ -integration of the SANS scattering curve obtained in absolute units allows for the determination of the scattering invariant, and this value can be compared to the calculated value from the chemical formula assuming that density of the polymer is 2.1 g/cm<sup>3</sup>. The same calculation has been performed assuming that the ionic groups either are located inside

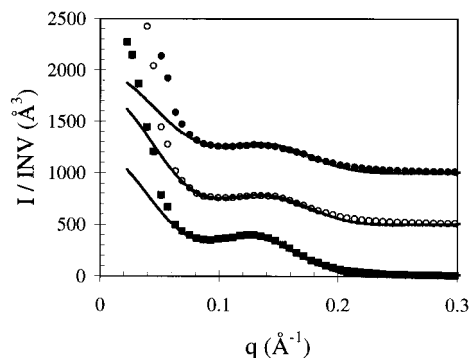


**Figure 4.** SAXS profiles of water-swollen EW = 909 (■), EW = 1076 (○), and 1269 (●) SPC PFSI. The solid lines correspond to the best fits using the local order model (parameters listed in Table 2). An offset (500 Å<sup>3</sup>) was applied between each curve for clarity.

the ionic domains or contribute to the scattering of perfluorinated matrix. In both cases the results are in excellent agreement with the calculated value since the difference between the two values is lower than the experimental error in the determination of the scattering invariant. This result indicates that the SAXS and SANS techniques are not able to differentiate between these two hypotheses due to the extremely large contrast between the fluorinated polymer matrix and the hydrogenated solvent. The fact that it is not necessary to take into account the localization of the fixed ions in the models significantly reduces the number of model parameters necessary to reproduce the scattering curves.

Geometrical considerations using space-filling arguments based on a diamond-like structure<sup>8</sup> permit the determination of the radius and the interaggregate distance from the peak position using eq 6 and  $D = 3d_{\max}/4$ . These values were determined for each membrane and used as starting value in the fitting procedure using the local order model (eq 4). Since the scattering maximum can be slightly shifted by the presence of the small-angle upturn in intensity at low angles, the value of the radius was adjusted. The value of the interaggregate distance was kept related to the radius value through eq 6. The values of  $z$  and  $\alpha$  were then refined to obtain the best fits. The results are presented in Figures 2 and 4 for the EW = 800, 909, 1096, and 1269 membranes. The agreements can be considered as excellent since both the shape and the intensity are reproduced. The values of  $R$ ,  $D$ ,  $z$ , and  $\alpha$  deduced from the fitting procedure are listed in Table 2, and several important features become apparent. First,  $d_{\max}$  decreases and  $D$  increases as EW increases while these values should be proportional ( $D = 3d_{\max}/4$ ). This is probably an effect of the presence of the crystalline component at low angles which shifts the scattering maximum. At large EWs, both the number of ionic groups per aggregate and the number of water molecules per ionic group are constant. Therefore, the radii of the aggregate dimensions are constant with varying EW as observed from both the Porod and the model analysis. It follows that the interaggregate distance should increase as deduced from the fit parameters. Second, the radii deduced from the model and from the Porod analysis are significantly different. This discrepancy is probably due to the presence of the crystallinity which acts on both values. The crystallinity increases as the ionic content decreases. For the Porod analysis, we have considered the intensity as originated from a two-phase system, and we have neglected a possible

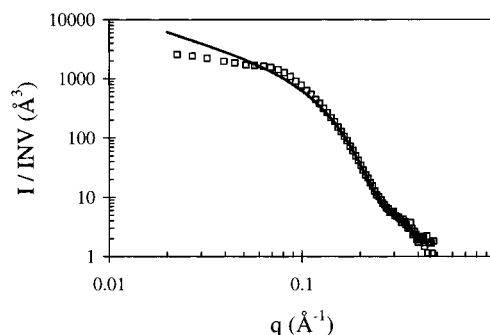


**Figure 5.** SAXS profile of water-swollen EW = 635 SPC PFSI (□). The solid line corresponds to the best fit using the form factor of polydisperse rodlike particles ( $R = 15 \pm 3$  Å).

contribution of the crystalline component to the total quantity of interface. The value of the specific surface appears to be overevaluated for large EWs, which leads to smaller values for the radii. The second effect of the crystalline component to the scattered intensity is to shift the ionomer peak toward smaller angles and to increase its intensity. Therefore, the fit, which mainly takes into account the peak position and its intensity, leads to overevaluated values of the radius. Moreover, the ionic domains are located in the amorphous phase. It follows that the local water volume fraction is significantly larger than the overall volume fraction, which can significantly modify the value of the fit parameters. The actual value of the radius is thus in between the two experimental values, and a realistic value is probably in the range of 15 Å.

The  $\alpha$  and  $z$  parameters act mainly on the small-angle upturn in intensity, and their variation with the EW is not relevant; however, it further confirms that the contribution of the crystalline component increases as EW increases. It can be noted that the values of the  $\alpha$  and  $z$  parameters found for LPC PFSI membranes ( $z = 4.45 \pm 0.05$  and  $\alpha = 1.155 \pm 0.005$ )<sup>8</sup> are very close to the ones determined in the present work.

The model was not able to fit the scattering curve obtained for the lowest EW membrane. This is due to the fact that the water uptake of the membrane is so large (80%) that the swollen membrane can no longer be considered as a water-in-polymer system, but rather as a polymer-in-water system as previously shown for highly swollen LPC PFSI membranes.<sup>16</sup> The previous studies of perfluorinated ionomer solutions have indicated that PFSI "solutions" are polymer dispersions of rodlike aggregates composed of a polymer core with the ionic groups located at the polymer-solvent interface.<sup>15,22</sup> These rodlike particles in water are formed during the dissolution process, and the small-angle scattering study of EW 800 SPC PFSI solutions allowed for the determination of a value of the radius  $R = 17$  Å. The structure of highly swollen PFSI membranes corresponds to a connected network of rodlike particles, and the SAXS profile obtained for the swollen EW = 635 SPC PFSI was tentatively reproduced by the form factor of cylinders. The scattering intensity at low  $q$  values is significantly altered by the presence of the interference term, but the agreement can be considered as excellent for large  $q$  values. This angular domain reflects the local structure on a scale of a few nanometers. The adjustment was performed with the form factor of cylinders introducing a Gaussian polydispersity (Figure 5). The radius is  $15 \pm 3$  Å, and the fitted polydispersity reflects the contribution of the nodes of the connected network

in addition to the radius dispersion. This radius value can be compared to the ones determined for the EW 800 SPC and the EW 1100 LPC PFSI solutions (respectively 17 and 25 Å). The volume of the rods should be related to the average volume associated with each ionic group,  $v_0$ . For rodlike particles, the packing parameter,  $v_0/(\sigma R)$ , is thus expected to be close to 0.5.<sup>23</sup> The values are 0.58, 0.62, and 0.63 for the SPC 635 swollen membrane, the SPC 800, and the LPC 1100 PFSI solutions, respectively. This result confirms the rodlike structure and indicates that the main parameter is the polymer volume associated with each ionic group rather than the pendant side chain length.

## Conclusions

The specific surface of water-swollen SPC PFSI membranes obtained from the analysis of the asymptotic behavior at large angles is found to be constant with varying the equivalent weight over a large range. This behavior confirms that the structure is dominated by interfacial phenomena. The scattering profiles obtained for dry membranes, room humidity, and water-swollen membranes are satisfactorily reproduced by the local order model. The radius varies from 15 to 25 Å, and the interdomain distance is roughly constant ( $D \approx 40$  Å) as the EW decreases from ca. 1300 to 800. For large ionic content (low EW), the degree of swelling is very large, and the swollen membrane can be analyzed as a connected rodlike network leading to 15 Å as value of the radius. We are aware that a good fit of the data with a model is not entirely sufficient to prove its validity without additional and independent convincing results obtained with different techniques. Such additional results perhaps could be obtained by electron microscopy or AFM analysis; however, such techniques have yet to provide conclusive results with ionomers and require specific developments that are under progress.

**Acknowledgment.** The authors thank the LLB for providing neutron beam time and José Teixeira as local contact.

## References and Notes

- (1) *Perfluorinated Ionomer Membranes*; Eisenberg, A., Yeager, H. L., Eds.; American Chemical Society: Washington, DC, 1982; Vol. 180.
- (2) *Ionomers: Characterization, Theory and Applications*; Schlick, S., Ed.; CRC Press: Boca Raton, FL, 1996.
- (3) *Modern Chlor-alkali technology*; Coulter, M. O., Ed.; Ellis Horwood: Chichester, England, 1980.
- (4) Longworth, R.; Vaughan, D. J. *Polym. Prepr. (Am. Chem. Soc., Div. Polym. Chem.)* **1968**, 9, 525.
- (5) Gebel, G.; Loppinet, B. In *Ionomers: Characterization, Theory and Applications*; Schlick, S., Ed.; CRC Press: Boca Raton, FL, 1996; pp 83–106.
- (6) Roche, E. J.; Pineri, M.; Duplessix, R. *J. Polym. Sci., Polym. Phys. Ed.* **1982**, 20, 107–116.
- (7) Gierke, T. D.; Munn, G. E.; Wilson, F. C. *J. Polym. Sci., Polym. Phys. Ed.* **1981**, 19, 1687–1704.
- (8) Gebel, G.; Lambard, J. *Macromolecules* **1997**, 30, 7914–7920.
- (9) Dreyfus, B.; Gebel, G.; Aldebert, P.; Pineri, M.; Escoubes, M.; Thomas, M. *J. Phys. (Paris)* **1990**, 51, 1341–1354.
- (10) Alexander, L. E. US patent, 1986.
- (11) Moore, R. B.; Martin, C. R. *Macromolecules* **1989**, 22, 3594–3599.
- (12) Heaney, M. D.; Glugla, P. G.; Martin, C. W.; Harthcock, M. A. Proceedings of the 33rd IUPAC, Montreal, 1990.
- (13) Halim, J.; Büchi, F. N.; Hass, O.; Stamm, M.; Scherer, G. G. *Electrochim. Acta* **1994**, 39, 1303–1307.
- (14) Porod, G. In *Small-Angle X-ray Scattering*; Glatter, O., Kratky, O., Eds.; Academic Press: London, 1982; p 17.
- (15) Loppinet, B.; Gebel, G. *Langmuir* **1998**, 14, 1977–1983.
- (16) Gebel, G. *Polymer* **2000**, 41, 5829–5838.
- (17) Dreyfus, B. In *Structure and Properties of Ionomers*; Pineri, M., Eisenberg, A., Eds.; D. Reidel Publishing Co.: Dordrecht, Holland, 1987; Vol. NATO ASI Ser. C-198; pp 27–37.
- (18) Roche, E. J.; Pineri, M.; Duplessix, R.; Levelut, A. M. *J. Polym. Sci., Polym. Phys. Ed.* **1981**, 19, 1.
- (19) Fujimura, M.; Hashimoto, T.; Kawai, H. *Macromolecules* **1981**, 14, 1309.
- (20) Gebel, G.; Aldebert, P.; Pineri, M. *Macromolecules* **1987**, 20, 1425–1428.
- (21) Litt, M. H. *Polym. Prepr.* **1997**, 38, 80–81.
- (22) Loppinet, B.; Gebel, G.; Williams, C. E. *J. Phys. Chem.* **1997**, 101, 1, 1884–1892.
- (23) Israelachvili, J. N.; Mitchell, D. J.; Ninham, B. W. *J. Chem. Soc., Faraday Trans. 2* **1976**, 72, 1525–1568.

MA9912709